ZIBELINE INTERNATIONAL PUBLISHING

ISSN: 2521-0890 (Print)
ISSN: 2521-0491 (Online)
CODEN: GBEEB6

Geological Behavior (GBR)

DOI: http://doi.org/10.26480/gbr.02.2020.78.83

RESEARCH ARTICLE

# INVESTIGATION OF SUBSURFACE STRUCTURES WITHIN PARTS OF NIGER DELTA, NIGERIA, VIA AEROMAGNETIC DATA

**Ekpa, Moses M. M[a]., Ibuot, Johnson C.[b]*, Okeke, Francisca N[b]. and [2]Obiora, Daniel N.[b]**

*[a] Federal College of Education (Technical), Omoku, Rivers State, Nigeria*
*[b] University of Nigeria, Nsukka, Enugu State, Nigeria*
**Corresponding author email: johnson.ibuot@unn.edu.ng*



**ARTICLE DETAILS**

***Article History:***

Received 10 March 2020
Accepted 12 April 2020
Available online 2 June 2020

**ABSTRACT**

Geophysical study involving aeromagnetic method was carried out to investigate parts of Niger Delta in Nigeria, aimed at investigating the cause and nature of anomalous bodies within the study area. Spectral analysis technique was employed in quantitative interpretation to determine depth/thickness of the sedimentary basin, basement topography, structural trends, curie point depth, thermal gradient and heat flow in the area. The total magnetic intensity (TMI) anomalies had values of between -53.7nT and 119.5nT while the residual magnetic intensity ranged from -52.5 to 58.0nT. The spectral analysis revealed the depth to magnetic sources varying from 2.5 to 5.5km while the shallow magnetic sources varied from 0.89 to 1.47km. The geothermal analysis revealed the curie point depth between 11.782 and 18.048km while the calculated geothermal gradient ranged lie between 32.137 and 49.231$^{o}Ckm^{-1}$. The heat flow values ranged from 80.343 to 123.080$mWm^{-2}$. The results from this study have thrown more light to the understanding of the variation of subsurface structures in the study area. These will enhance the development of the resources and will be of economic benefit to the country if well harnessed. However, possible future research work on this active area is proposed for more robust results.

**KEYWORDS**

Aeromagnetic, Niger Delta, curie point, heat flow, geothermal, basement.

## 1. INTRODUCTION

Aeromagnetic survey helps in detecting rocks or minerals with unusual magnetic properties that reveal themselves by causing disturbances or anomalies in the intensity of the earth's magnetic field. The principle involve in aeromagnetic survey is similar to ground magnetic survey but allows much larger areas of the Earth's surface to be covered speedily for regional reconnaissance. Different subsurface materials can cause local disturbances in the Earth's magnetic field which can be detected with sensitive magnetometers (Obiora et al., 2015; Oha et al., 2016). Aeromagnetic survey maps the variation of the geomagnetic field, which occurs due to changes in the percentage of magnetite in the rock and reflects the variations in the distribution and type of magnetic minerals below the earth surface and measure variations in basement susceptibility. Magnetics is useful wherever object of investigation has a contrast in magnetic susceptibility which varies from place to place beneath the earth surface. The magnetic data give insight into mapping of basement structures and delineating shallower volcanic materials etc. The characteristics of magnetic anomaly results from one or more physical parameters such as the configuration of the anomalous zone, magnetic susceptibility contrasts as well as the depth to the anomalous body.

According to a study, rock susceptibility is almost directly related to the percentage of magnetite present (Hassanein and Solimon, 2009). Many rocks in the earth subsurface exhibit magnetic properties, the magnetic properties of the Signatures, result from one or more physical parameter. The magnitude of the anomalies is related to the intensity of magnetization, size and position of the disturbing (Dopamu et al., 2011). These properties can be studied and mapped via ground or airborne magnetic survey. The airborne magnetic survey helps in covering large areas rapidly in order to define targets for more cost and time-consuming exploration activities like seismic. Aeromagnetic survey maps the variation of the geomagnetic field, which occurs due to changes in the percentage of magnetite in the rocks. It reflects the variations in the distribution and type of magnetic minerals below the earth surface. It equally recognizes structures like faults, lineaments and measure variations in basement susceptibility (Arymanesh, 2009; Adetona et al., 2013; Abbas and Mallam, 2013; Sunmonu and Alagbe, 2014).

The mapped anomalies are correlated with the underlying geological structures of the study area, since the knowledge of geology is the scientific basis for any geophysical exploration. Depth to basement is important in exploration particularly for the determination of areas where there may be mature hydrocarbon. According to a study, the applications of aeromagnetic method play an important role in tracing lithological contacts and to recognize the structures like faults, lineaments, dykes and layered complexes which may have influence on the overlying sediments (Arymanesh, 2009). Magnetic method is important in oil exploration because it helps in the estimation of the sedimentary thickness from the depth of the magnetic basement. The objectives of this study are to interpret the aeromagnetic data in order to determine the sedimentary thickness of the study area, determine the depth to magnetic basement and to interpret the magnetic anomalies revealed by the aeromagnetic map, delineate the basement topography, infer the structural variations and structures within the study area.

| Quick Response Code | Access this article online | |
|---|---|---|
| | Website: www.geologicalbehavior.com | DOI: 10.26480/gbr.02.2020.78.83 |

Cite the Article: Ekpa, Moses M. M., Ibuot, Johnson C., Okeke, Francisca N. and Obiora, Daniel N. (2020). Investigation Of Subsurface Structures Within Parts Of Niger Delta, Nigeria, Via Aeromagnetic Data. *Geological Behavior, 4(2): 78-83*

### 1.1 Location and geology of the study area

The Niger Delta Basin is situated in the Gulf of Guinea (Tuttle et al., 1999). It is one of the most prolific hydrocarbon basins in the world. The Niger Delta has an area of 300,000km$^2$, sediment thickness of over 10,000km and sediment volume of 500,000km$^3$ (Okiwelu and Ude, 2013). The study area (Figure 1) lies between latitudes 3°30' – 4°00'N, longitude 6°00' – 7°00'E (offshore) and latitude 4°00' – 4°30'N, longitude 6°30' – 7°00'E (onshore). The Niger Delta sediments are divided into three distinct units of Eocene to Recent ages that form major transgressive and regressive cycles. The Niger Delta generally displays three vertical lithostratigraphic subdivisions: an upper delta top facies; a middle delta front lithofacies; and a lower pro-delta lithofacies. These lithostratigraphic units correspond respectively with the continental sands of Benin Formation (Oligocencene-Recent), the alternating sand/shale paralic of Agbada Formation (Eocene-Recent) and the marine prodelta shales of Akata Formation (Paleocene-Recent). The sands and sandstones of Agbada formation are the main hydrocarbon reservoirs. The shape and internal structure of the Niger Delta are also controlled by fracture zones along oceanic crust. The Niger delta sits at the southern end of Benue trough, corresponding to a failed arm of rift triple junctions (Lehner and De Ruiter, 1977).

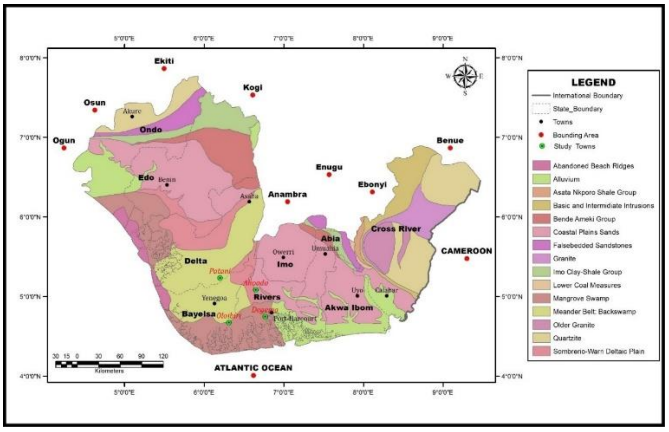


**Figure 1:** Map showing the location and geology of the study area

## 2. METHODS

Magnetic method is generally complex and variations in the magnetic field are more erratic and localized. This is partly due to the difference between the dipolar magnetic field and partly due to the variable directions of the magnetic field. Magnetic data in recent years has been expanded beyond being tools for basement mapping to include modeling of prospect-level targets (Kearey and Brooks, 2004; Omeje et al., 2012). The spatial variations in the physical properties (magnetic susceptibility) of rocks changes significantly from one rock to another (Lowrie, 2007). The magnetic method is based on Coulomb's law which is given mathematically as in eq.(1);

$$F = \frac{\mu_0 P_1 P_2}{4\pi r^2} \quad (1)$$

Where $\mu_0$ is the magnetic permeability constant for free space.

The magnetic field B is defined as the force exerted by a pole of strength P on a unit pole at distance r and is given by eq. (2);

$$B = \frac{\mu_0 P}{4\pi r^2} \quad (2)$$

Magnetic susceptibility (k) which determines how much magnetization will be present due to external magnetic field relates the intensity of magnetization (I) to the strength of the induced magnetic field (H) and is represented by eq. (3).

$$K = \frac{I}{H} \quad (3)$$

Four digitized aeromagnetic sheets of Olobirin (sheet 327), Degema (sheet 328), Patani (sheet 319) and Ahoada (sheet 320) presented in XYZ Geosoft format were acquired, analyzed and interpreted. The data were gridded using minimum curvature method (Briggs, 1974; Swain, 1976; Webring, 1981) and the gridding produces total magnetic intensity (TMI) grid. The qualitative interpretation is the preparation of the potential field maps or grids on which the anomalous values at different stations are plotted and on which contours are drawn at suitable intervals. The contour maps were generated using Oasis Montaj software by interpolation. Mathematical filters were employed in quantitative interpretation of the data using different filtering methods such as Polynomial fitting, reduction to pole (RTP), first vertical derivative (FVD), second vertical derivative (SVD) and horizontal derivative (HD).

The spectral depth method is based on the principle that a magnetic field measured at the surface could be considered as an integral of magnetic signature from all depths and Discrete Fourier Transform is the mathematical tool for spectral analysis (Rabeh, 2009). This is applied to regularly spaced data such as the aeromagnetic data. In estimating the depth to basement from spectral analysis, the study area was subdivided into equal spectral blocks using the filtering tools of the Microsoft excel software. This transforms the magnetic data into the radial energy spectrum for each block. The average radial energy spectrum calculated is displayed in a logarithm figure of energy versus frequency. Two linear segments are drawn from each graph; and their gradients (m) were employed in estimating the deep depth ($D_1$) and the shallow depth ($D_2$) using eqs. (4), (5) and (6) respectively (Hahn et al., 1979; Connard et al., 1979).

$$\text{Slope } (m_1, m_2) = \frac{\text{Log Energy}}{\text{Frequency}} \quad (4)$$

$$D_1 = -\frac{m_1}{2\pi} \quad (5)$$

$$D_2 = -\frac{m_2}{2\pi} \quad (6)$$

Where $m_1$ and $m_2$ are slopes of the first and second segment of the plot and the negative sign (-) indicates depth to the subsurface.

Curie point depth which is the deepest level in the earth crust and contain materials which create discernible signatures in a magnetic anomaly map (Bhattacharyya and Leu, 1975). This point is assumed to be the depth for the geothermal source where most geothermal reservoirs tapped their heat and offers a window for a better view of the thermal structure of the crust. To perform the analysis, Microsoft excel and FOURPOT software were employed and graphs of the logarithms of the spectral energies against frequencies were plotted for the various blocks, two linear segments were drawn from each graph; and their gradients were used to calculate the depth to the centroid ($Z_0$) and the depth to the top boundary ($Z_t$) using eqs.(7),(8)and (9) respectively. The Curie point depth ($Z_b$) was calculated using eq. (10) (Okubo et al., 1985; Tanaka et al., 1999; Eletta and Udensi., 2012).

$$\text{Slope } (m_1, m_2) = \frac{\text{Log Energy}}{\text{Frequency}} \quad (7)$$

$$Z_0 = -\frac{m_1}{2\pi} \quad (8)$$

$$Z_t = -\frac{m_2}{2\pi} \quad (9)$$

Where $m_1$ and $m_2$ are slopes of the first and second segment of the plot and the negative sign (-) indicates depth to the subsurface.

$$Z_b = 2Z_0 - Z_t \quad (10)$$

Geothermal gradient is the rate of increase in temperature per unit depth in the earth due to the outflow of heat from the center and helps in determining suitable places for siting geothermal plants for the generation of electricity that can be utilized for industrial, domestic and recreational activities. The geothermal gradient within the earth's surface is defined by eq. (11) (Frost and Shive, 1986; Stampolidis et al., 2005; Maden, 2010).

$$\left[\frac{dT}{dZ}\right] = \frac{\theta}{Z_b} \quad (11)$$

where $\theta = 580°C$ is the Curie temperature for magnetite. Laboratory experiments showed that ferromagnetic materials lose their magnetism above the Curie temperature (580°C) because the thermal energy is sufficient to maintain a random alignment of the magnetic moments of the iron minerals (Hinze et al., 2013; Tanaka et al., 1999). The relationship between the Curie isotherm depth ($Z_b$) and the heat flow (q) is given by eq.(12) (Turcotte and Schubert, 1982; Tanaka et al., 1999; Nwankwo et al., 2011);

$$q = \sigma\left[\frac{\theta}{Z_b}\right] \quad (12)$$

Where $\sigma = 2.5 Wm^{-1}°C^{-1}$ is the average thermal conductivity.

## 3. Results and Discussion

The data was gridded in order to produce the total magnetic intensity (TMI) map of the study area (Figure 2). Areas of strong positive anomalies likely indicate a higher concentration of magnetically susceptible minerals and areas with magnetic lows may be areas of low magnetic concentration and therefore lower susceptibility. The range of TMI (-53.7nT to 119.5nT) shows that the study area is magnetically heterogeneous.

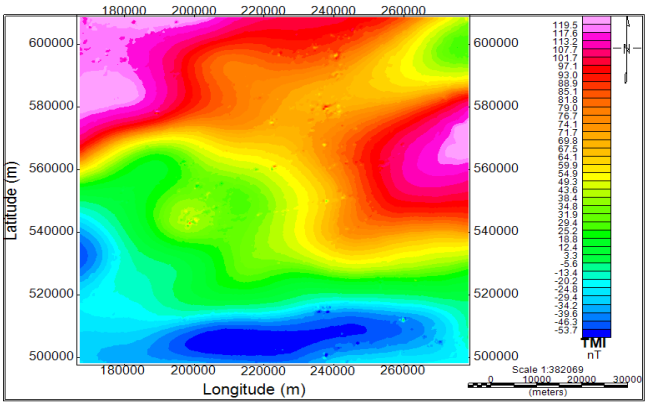


**Figure 2:** Total magnetic intensity (TMI) map of the study area

The separation of residual and regional field from the potential field data was done by applying a first order polynomial using Oasis Montaj™ software. The residual map (Figure 3) revealed that the magnetic field intensity ranges from -52.5nT to 58.0nTindicatingcharacteristic low and high magnetic signature.

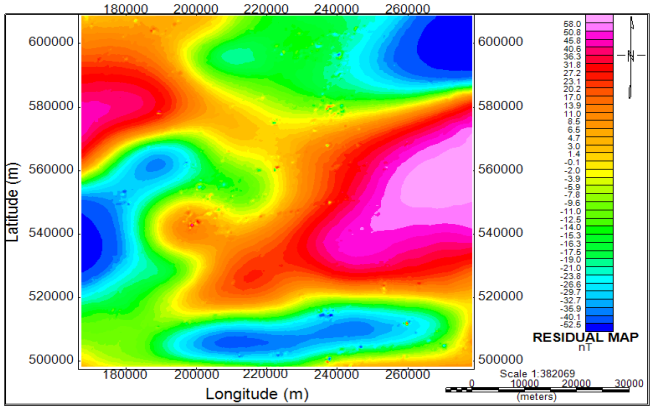


**Figure 3:** Residual magnetic map of the study area.

Figure 4 is the regional magnetic intensity map of the study area with values ranging from 28.2nT to 114.0nT. The values decrease from north to south indicating there is a fill of sediments more in the southern part than in the northern part of the study area. Figures 5 is the horizontal derivative computed from the residual magnetic intensity gridusing Oasis montaj™ software. The horizontal derivative shows more exact location for faults and the fault lines can be seen clearly on the magnetic lineament map (Figure 6). The magnetic lineament map shows the region is fragmented by features such as outcrops, cracks, fractures, faults and joints all serve as reservoir for the suspected minerals in the study area. The lineament patterns are favorable conditions in control of various mineral deposits in Niger Delta (Emujakporue and Ofoha, 2015).

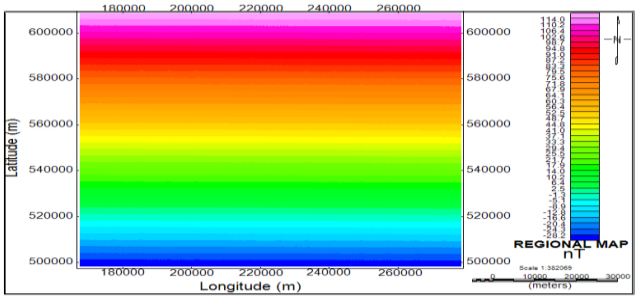


**Figure 4:** Regional Magnetic Intensity Map of the study area

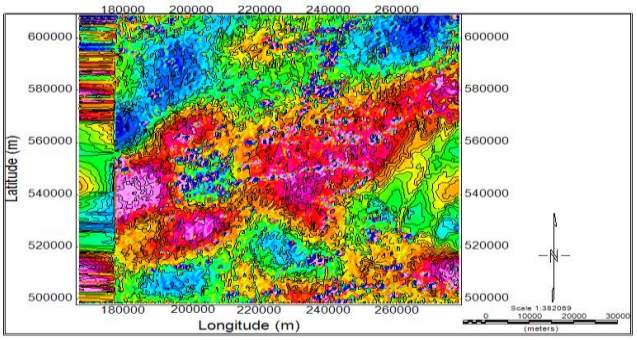


**Figure 5:** Aeromagnetic horizontal derivative map of the study

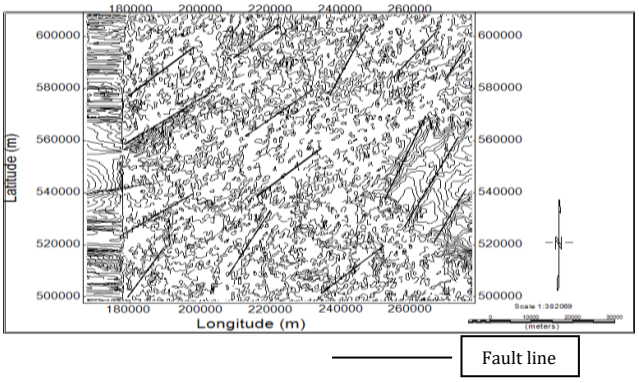


**Figure 6:** Magnetic lineament map showing the lines of the faults in the study area.

Spectral analysis was employed in estimating the depth to basement, delineating the basement topography, estimating the curie point depth, geothermal gradient and the heat flow in the area. The study area was subdivided into twenty-five equal spectral blocks (Figure 7) using the filtering tool of the Microsoft excel software. Each block covers a square area of 22km by 22km in order to accommodate longer wavelength so that the depth to the basement up to about 6km could be investigated.

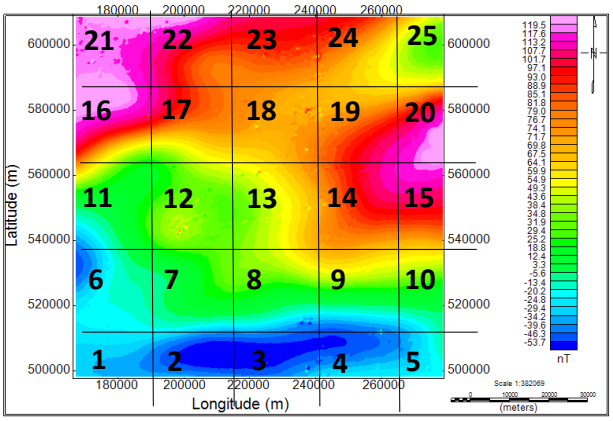


**Figure 7:** Twenty-five spectral blocks for estimation of the depth to basement.

Microsoft (MS) excel program employing the Fast Fourier Transform (FFT) technique was employed in transformation of magnetic data into the radial energy spectrum for each block. The average radial energy spectrum was calculated and displayed in a logarithm figure of energy versus frequency. The Log-energy spectrum with linear gradient magnitude is dependent upon the depth of the source (Spector and Grant, 1970; Hahn et al., 1979; Spector and Grant, 1970). Graphs of radial average energy spectrum were plotted as Log of Energy versus Frequency in radian per meter. Graphs were plotted for the 25 spectral blocks as shown in Figure8. For each block, two linear segments could be identified which implies that there are two magnetic source layers in the study area. The gradient of each of the line segments were first evaluated and the deep (red line) and shallow (black line) depth were calculated. The two depth estimates for each of the twenty-five spectral blocks give a range of 2.488 to 4.777 with an average of 3.950 for the deep depth (D1) and 0.885 to 1.468 with an average of 1.087 for the shallow depth (D2).

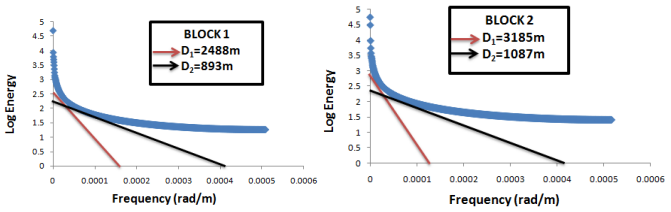


**Figure 8:** Spectral plots of logarithm of Energy against Frequency (radian per meter).

Employing surfer 10 software in plotting and contouring the magnetic basement depth, revealed that the deep magnetic sources vary between 2.5 and 5.5km (Figure 9), whereas the shallow magnetic source varies between 0.89 and 1.47km (Figure 10). The earlier suggests depth to precambrian basement while the later suggests depths to basic intrusive and/or magnetised bodies. The depth to basement is shallowest in the southwestern part of the study area, while it is deepest in the north eastern part. From the 3D surface map of the area (Figure11), a linear depression with thickest sediments is observed at the north eastern part of the study area, while an elevation with shallowest sediments is observed at the southwestern part of the study area. The irregular nature of the basement may be attributed to faults that aid the migration and entrapment of hydrocarbon and other mineralized deposits in line with findings of (Ako et al., 2014).

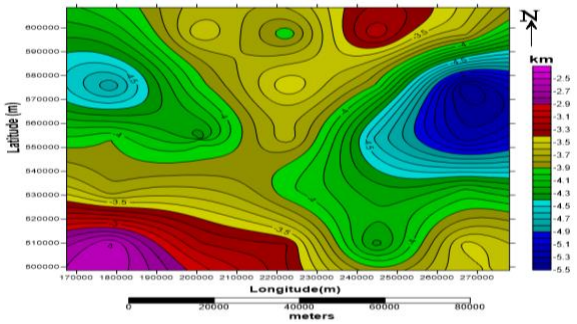


**Figure 9:** Deep depth to basement map.

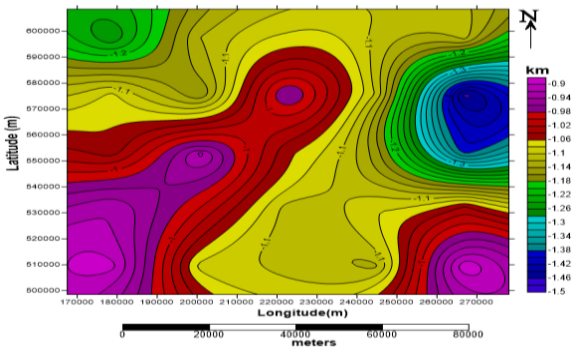


**Figure 10:** Shallow depth to basement map.

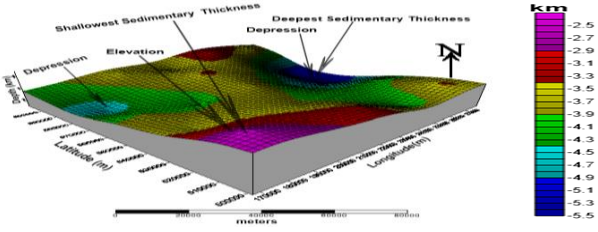


**Figure 11:** 3D map of the study area showing magnetic basement topography.

In estimating the curie point depth, geothermal gradient and heat flow, the study area was subdivided into sixteen equal spectral blocks (Figure 12) using the filtering tool of the Microsoft Excel software. Each block covers a square area of 55km by 55km in order to accommodate longer wavelength, so that depth to the centroid greater than 6km could be investigated.

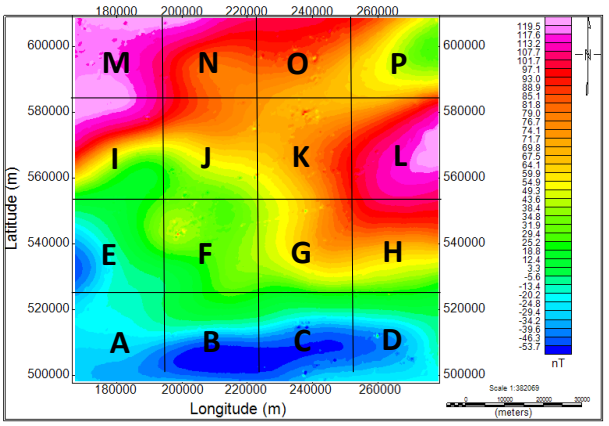


**Figure 12:** Sixteen spectral blocks for geothermal analysis.

The magnetic data were transformed into radial energy spectrum for each block and the average radial energy spectrum was calculated and displayed in a logarithm plot of energy versus frequency, as could be seen in Figure 13. For each block, two linear segments could be identified which implies that there are two magnetic source layers in the study area.

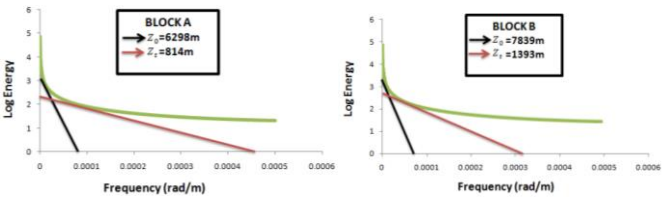


**Figure 13:** Spectral plots of logarithm of Energy against Frequency

The gradient of each of the line segments were first evaluated and the depth to Centroid, $Z_0$ (black line) and depth to top boundary, $Z_t$ (red line) were calculated. The Curie point depth ($Z_b$), thermal gradient ($\frac{dT}{dz}$) and the heat flow (q) of the study area were calculated (Table 1). The 2D Curie isotherm depth (Figure 14), the geothermal gradient and heat flow contour maps of the study area (Figures 15 and 16) respectively were generated. Figure 15shows the Curie point depth of the study area to range from 12km to 18km. This reveals that the deepest curie point depth lies at the north east while the shallowest is found at the south western part of the study area. The geothermal gradient ranges from 32.137°C/km to 49.231°C/km with an average value of 39.317°C/km (Table 1) indicating possibility for hydrocarbon generation. It is observed that region with significant geothermal energy is characterized by an anomalous high temperature gradient and heat flow. The geothermal gradient map (Figure 15) depicts areas of lowest, intermediate and highest geothermal gradient values. Areas with geothermal gradients above 40°C/km may be prospective for geothermal energy development from which electricity may be generated.

**Table 1:** Calculated Curie depth, Geothermal gradient and Heat flow

| BLOCKS | Depth to Centroid ($Z_0$) km | Depth to top boundary ($Z_t$) km | Curie Depth ($Z_b$) km | Geothermal gradient ($\frac{dT}{dz}$) °C/km | Heat Flow(q) $mWm^{-2}$ |
|---|---|---|---|---|---|
| A | 6.298 | 0.814 | 11.782 | 49.231 | 123.080 |
| B | 7.839 | 1.393 | 14.285 | 40.602 | 101.505 |
| C | 7.583 | 0.995 | 14.171 | 40.929 | 102.323 |
| D | 7.349 | 1.077 | 13.621 | 42.581 | 106.453 |
| E | 7.682 | 0.796 | 14.568 | 39.813 | 99.533 |
| F | 7.723 | 0.857 | 14.589 | 39.756 | 99.390 |
| G | 7.962 | 0.936 | 14.988 | 38.698 | 96.745 |
| H | 8.530 | 1.720 | 15.340 | 37.810 | 94.525 |
| I | 8.107 | 1.013 | 15.201 | 38.155 | 95.388 |
| J | 8.381 | 1.171 | 15.591 | 37.201 | 93.003 |
| K | 8.084 | 2.171 | 13.997 | 41.437 | 103.593 |
| L | 9.820 | 1.592 | 18.048 | 32.137 | 80.343 |
| M | 8.404 | 1.960 | 14.848 | 39.063 | 97.658 |
| N | 8.574 | 1.539 | 15.609 | 37.158 | 92.895 |
| O | 8.758 | 1.601 | 15.915 | 36.444 | 91.110 |
| P | 8.614 | 1.990 | 15.238 | 38.063 | 95.158 |
| Average | | | 14.862 | 39.317 | 98.294 |

The heat flow values range from 80.343$mWm^{-2}$ to 123.080$mWm^{-2}$ with an average value of 98.294 $mWm^{-2}$ (Table 1). Figure 16 shows the variation of heat flow in study area with the highest heat flow observed in the southwestern part of the study area and the lowest heat flow found around northeastern part of the study area. It can be inferred that the regions with high and low geothermal gradient corresponds with the regions with high and low heat flow. This is consistent with the values of Curie point depth observed in the area. The quantitative change in Curie depth implies that, the heat flow in the study area is not uniform. The plot (Figure 17) shows that heat flow is inversely proportional to the Curie depth indicating that the heat flow in the study area increases with decreasing Curie isotherm depth

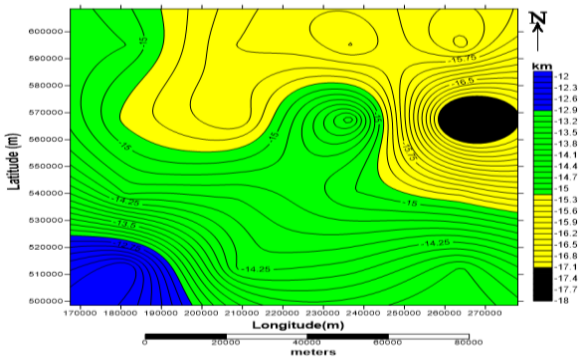


**Figure 14:** Curie depth map of the study area.

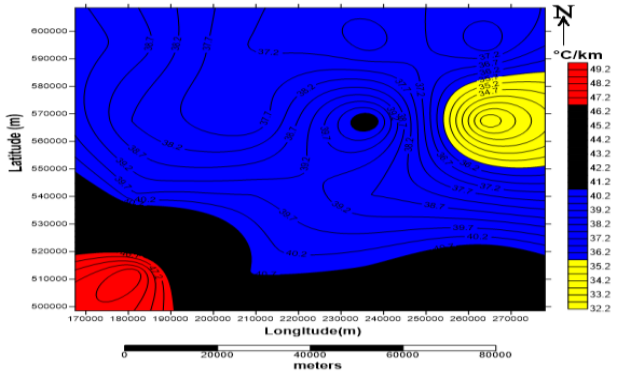


**Figure 16:** Geothermal gradient contour map of the study area.

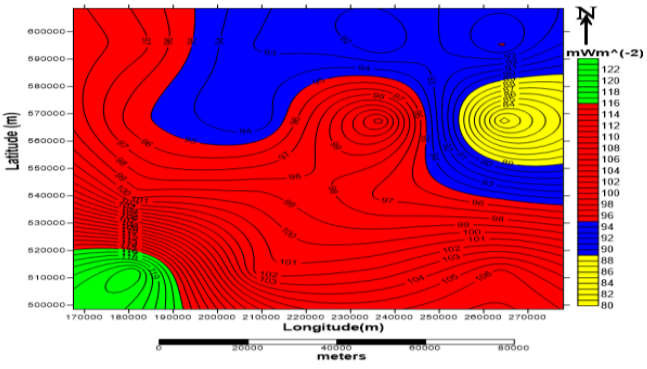


**Figure 17:** Heat flow contour map of the study area.

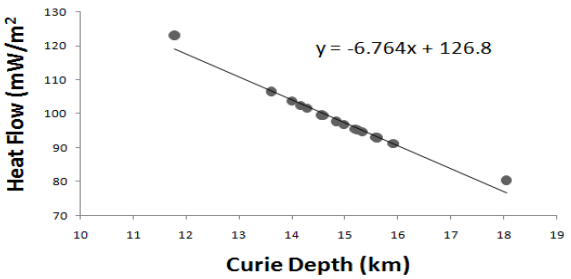


**Figure 18:** Plot of heat flow against Curie point depth

## 4. Conclusion

From the geophysical investigation of parts of Niger Delta in Nigeria carried out using aeromagnetic data, there is clear evidence from the results of total magnetic intensity and residual magnetic intensity that the study area is magnetically heterogeneous. The structural trend map which was derived from the aeromagnetic horizontal vertical derivative indicates the presence of faults in the study area. Our results support the notion that the values registered for average geothermal gradient of suggests possibility of hydrocarbon generation in the study area. Furthermore, the obtained geothermal gradients value of 49.231°C/km suggests a prospective area for geothermal energy development. Hence, these possibilities definitely add to the existing knowledge on investigation of subsurface structures in parts of Niger Delta, Nigeria.

## References

Abbas, A.A., Mallam, A., 2013. Investigating the structures within the lower Benue and upper Anambra basins, Nigeria, using first vertical derivative, analytical signal and (CET) center for exploration targeting plug-in. Earth Science, 2, Pp. 104-112.

Adetona, A., Abbass, A., Mallam, A., 2013. Investigating the structures within the Lower Benue and Upper Anambra Basins, Nigeria, using first vertical derivative, analytical signal and (CET) center for exploration targeting Plug-in. Earth Science, 2, Pp. 104-112.

Ako, B.D., Ojo, S.B., Okereke, C.S., Ajayi, T.R., Adepelumi, A.A., Afolayan, J.F., Afolabi, O., Ogunnusi, H.O., 2014. Some observations from gravity/magnetic data interpretation of the Niger Delta.Nigeria Association of Petroleum Explorationist Bulletin, 17, Pp. 11-12.

Arymanesh, M., 2009. Aeromagnetic data interpretation to locate buried faults in Yazd province– Iran. World Applied Sciences Journal, 6, Pp. 1429-1432.

Bhattacharyya, B.K., Leu, L.K., 1975. Spectral Analysis of Gravity and Magnetic anomalies due to two-dimensional structure. Geophysics, 40, Pp. 993 –1013.

Briggs, I.C., 1974. Machine contouring using minimum curvature. Geophysics, 39, Pp. 39-48.

Connard, G., Couch, R., Gemperte, M., 1983. Analysis of aeromagnetic measurements from the Cascade Range in Central Oregon. Geophysics, 48, Pp. 376-390.

Dopamu, K.O., Nwankwo, L.I., Olatunji, S., Akoshile, C.O., 2011. Estimation of magnetic source depth from aeromagnetic data of Bida using gradient invasion method. International Journal of Physical Science, 3, Pp. 115-120.

Eletta, B.E., Udensi, E.E., 2012. Investigation of the Curie point Isotherm from the Magnetic Fields of Eastern Sector of Central Nigeria. Geosciences, 2, Pp. 101-106.

Emujakporue, G., Ofoha, C.C., 2015. Spectral Depth Estimate of subsurface Structures over Parts of Offshore Niger Delta, Nigeria. The International Journal of Engineering and Science, 4, Pp. 42-53.

Frost, B.R., Shive, P.N., 1986. Magnetic mineralogy of the lower continental crust. Journal of Geophysical Research, 91, Pp. 6513–6521.

Hahn, A., Kind, E.G., Mishra, D.C., 1979. Depth estimation of magnetic sources by means of Fourier Amplitude spectra. Geophysics Prospecting, 24, Pp. 287-318.

Hassanein, H.J.E., Soliman, K.S. 2009. Aeromagnetic data interpretation of Wadi Hawashiya area for identitying surface and subsurface structures, North eastern desert, Egypt. Earth Science, 20, Pp. 117-139.

Hinze, W.J., VonFrese, R.R.B., Saad, A.H., 2013. Gravity and magnetic exploration. Cambridge University Press, Pp. 512.

Kearey, P., Brooks, M., 2004. An Introduction to Geophysical Exploration. Blackwell Scientific Publications, Pp. 296.

Lehner, D., De Ruiter, P.A.C., 1977. Structural history of Atlantic margin of Africa. AAPG Bulletin, 61, Pp. 961 – 981.

Lowrie, W., 2007. Fundamentals of Geophysics. Cambridge University Press, London.

Maden, N., 2010. Curie-point depth from spectral analysis of magnetic data in Erciyes stratovolcano (central Turkey). Pure and Applied Geophysics, 167, Pp. 349-358.

Nwankwo, L.I., Olasehinde, P.I., Akoshile, C.O., 2011. Heat flow anomalies from the spectral analysis of Airborne Magnetic data of Nupe Basin, Nigeria. Asian Journal of Earth Sciences, 1, Pp. 1-6.

Obiora, D.N., Ossai, M.N., Okwoli, E., 2015. A case study of aeromagnetic data interpretation of Nsukka area, Enugu state, Nigeria, for hydrocarbon exploration. International Journal of Physical Sciences, 10(17), Pp. 503-519.

Oha, I.A., Onuoha, K.M., Nwegbu, A.N., Abba, A.U., 2016. Interpretation of high-resolution aeromagnetic data over southern Benue Trough, southeastern Nigeria. Journal of Earth System Science, 125(2), Pp. 369–385.

Okiwelu, A.A., Ofrey-Kulo, O., Ude, I.A., 2013. Interpretation of regional magnetic data offshore Niger Delta reveals relationship between deep basement architecture and hydrocarbon target. Earth Science Research, 2, Pp. 13-32.

Okubo, Y.J., Graf, R., Hansen, R.O., Ogawa, K., Tsu, H., 1985. Curie point depth of the Island of Kyushu and surrounding areas. Japan Geophysic, 53, Pp. 481-491.

Omeje, M., Ibrahim, N. B., Meluda, O., Ugwoke, P.E., 2012. 2-Dmodelling of the major structures underlying Dong and Shellieng of upper Benue valley, using GM-SYS computer modelling. Journal of Natural Science Research, 2, Pp. 50.

Rabeh, T., 2009. Prospecting for the ferromagnetic mineral accumulations using the magnetic method at the Eastern Desert, Egypt. Journal of Geophysics and Engineering, 6, Pp. 401-411.

Spector, A., Grant, F., 1970. Statistical models for interpreting aeromagnetic data. Geophysics, 35, Pp. 293-302.

Stampolidis, A., Kane, I., Tsokas, G.N., Tsourlos, P., 2005. Curie point depths of Albania inferred from ground total field magnetic data. Surveys in Geophysics, 26, Pp. 461-480.

Sunmonu, L.A., Alagbe, O.A., 2014. Interpretation of Aeromagnetic Data of Kam, Using Semi-Automated Techniques. International Research Journal of Earth Sciences, 2, Pp. 1-18.

Swain, C.J., 1976. A FORTRAN IV program for interpolating irregularly spaced data using the difference equations for minimum curvature, Computers and Geosciences, 1, Pp. 231-240.

Tanaka, A., Okubo, Y., Matsubayashi, O., 1999. Curie point depth based on spectrum analysis of the magnetic anomaly data in East and Southeast Asia. Tectonophysics, 306, Pp. 461–470.

Turcotte, D.L., Schubert, G., 1982. Geodynamics: Applications of continuum physics to geological problems. Cambridge University Press, New York, Pp. 450.

Tuttle, M.L.W., Charpentier, R.R., Brownfield, M.E., 1999. The Niger Delta petroleum system: NigerDelta province, Nigeria, Cameroun and Equatorial Guinea, Africa, U. S. Geological Survey Open-file Report-99-50-H, 31P.

Webring, M., 1981. MINC: a gridding program based on minimum curvature. U.S. Geological Survey, 43, Pp. 81-1224.